NORSAR

NORSAR Scientific Report No. 1-1999/2000

Semiannual Technical Summary

1 April - 30 September 1999

Kjeller, November 1999

6.2 Continuous assessment of upper limit M_S

Introduction

The continuous seismic threshold monitoring technique (TM) is used to provide a continuous assessment of the size of events that may have occurred in a given geographical area. The main application of this technique has until now been restricted to short-period seismic data, both at regional and teleseismic distances.

We have recently initiated an effort to apply the continuous TM technique to long-period data, for the purpose of obtaining a continuous assessment of surface wave magnitude (M_S). In principle, this application is straightforward, but in practice one has to take into account many factors, not all of which apply to the short-period case, such as surface wave dispersion, oceanic versus continental propagation paths, the difficulties in calculating surface wave magnitudes at regional distances, regional calibration formulas for *log(A/T)* vs. *log(STA)* and so on.

Nevertheless, the TM application promises to significantly improve monitoring of surface waves. One of the main considerations of TM is that it provides a realistic estimate of network detection thresholds during "unusual" noise conditions, such as in the coda of a large earthquake or during a large aftershock sequence. In the short-period case, we have demonstrated that the global detection capability can deteriorate significantly for many tens of minutes following a large earthquake. In the long-period case, this situation could be expected to be far worse, since surface waves from a large earthquake can last for many hours.

We present initial results from investigating the relation between PIDC station magnitudes and STA based estimates calculated from bandpass filtered data, as well as a case study with monitoring of surface waves from a mining area on the Kola peninsula during and after a M_S 7.6 earthquake.

TM measurements of M_S

When developing a strategy for threshold monitoring of surface waves, we have used the automatic surface wave measurements at the PIDC as the basis. Their procedure consists of the following steps:

- Shape Rayleigh wave observations to a common response type (KS36000)
- Search window for Rayleigh waves derived from regionalized group velocity windows
- Measure largest *A/T* with periods between 18 and 22 seconds
- Calculate station magnitudes using relation of Rezapour and Pearce (1998)

$$M_S = \log(A/T) + \frac{1}{3}\log(\Delta) + \frac{1}{2}\log(\sin(\Delta)) + 0.0046\Delta + 2.730$$

Our experience with threshold monitoring of body waves has shown that short-term averages (*STAs*) can efficiently be used to represent the traditional *A/T* measurements used for magnitude estimation. We will therefore attempt to adopt a similar procedure for surface waves. Concerning the search window for Rayleigh waves, the PIDC calculate these from a regionalized group velocity model. Currently we do not have this utility at hand and we have therefore chosen to analyze surface wave travel-time observations available in the PIDC database to derive

the STA search windows. For threshold monitoring of surface waves we have established the following procedure:

- Bandpass filter data between 17 and 24 seconds, zero phase Butterworth of 2nd order
- Generate short-term averages (*STAs*) with a window length of 30 seconds
- Measure largest *STA* within a search window derived from empirical PIDC data
- Derive *A/T* equivalent from the *STA* observation using station dependent empirical relations between $log(A/T)_{KS36000}$ and *log(STA)*
- Calculate station magnitudes using relation of Rezapour and Pearce (1998)

In Fig. 6.2.1 we show the travel-times and group velocities of PIDC M_S measurements at ARCES for continental propagations paths. Notice that a search window spanning the 2.5-3.3 km/s group velocity window covers all observations at ARCES.

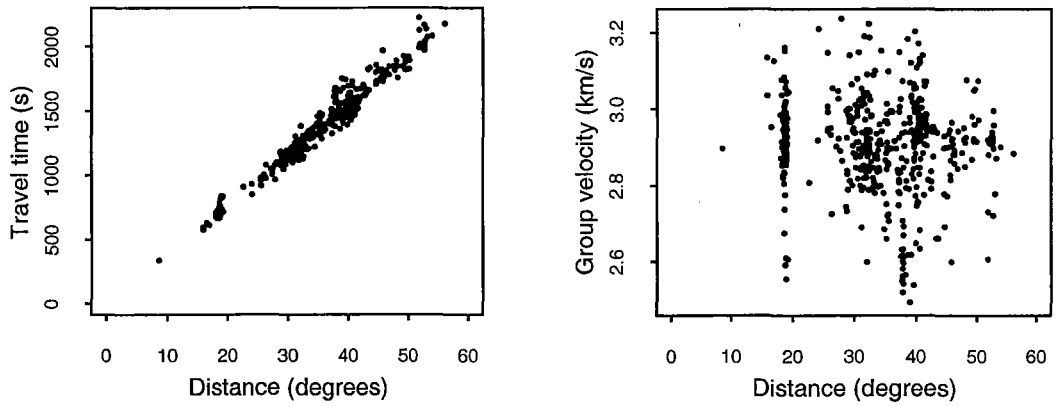

Fig. 6.2.1. *Travel-times and group velocities of PIDC M_S measurements at ARCES for continental propagations paths.*

Fig. 6.2.2 shows the relation between a small set of manual *log(A/T)* measurements made on the ARCES KS-36000 instrument, and *log(STA)* made on the same data filtered between 17 and 24 seconds. The difference between *log(A/T)* and *log(STA)* has a scatter with a standard deviation of 0.11 for this small data set, which is satisfactory in view of the scatter inherent in the magnitude-distance relation for surface waves (Rezapour and Pearce, 1998).

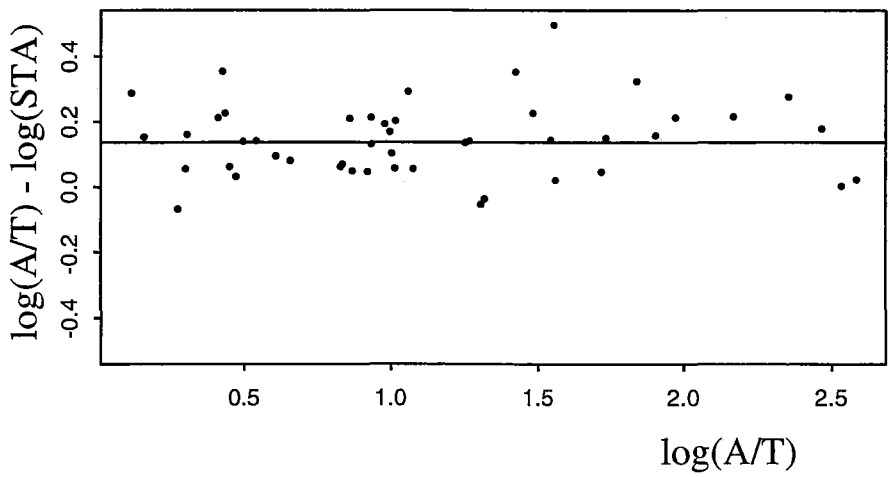

Fig. 6.2.2. Difference between manual log(A/T) measurements made on the ARCES KS-36000 instrument, and log(STA) made on the same data filtered between 17 and 24 seconds.
X-axis: log (A/T). Y-axis: $log(A/T)_{KS36000} - log(\frac{\pi}{2} \cdot STA \cdot \frac{cal_{20}}{20})$, *where* cal_{20} *is the-sensitivity in nm at 20 seconds.*

A first surface wave threshold monitoring experiment

As an example of TM processing of surface wave data, we have selected 17 August 1999, which was the day of the large Turkey earthquake (M_S=7.6). This earthquake was followed by numerous aftershocks, and therefore presents a good opportunity to assess the effects of such a situation on the surface wave detection capability. We focus our investigation on surface waves observed at the three Norwegian IMS stations NOA, ARCES and SPITS, as well as a TM trace based upon joint processing of the data from these three stations.

We have chosen to show a site-specific approach, with a TM beam focused towards the Lovozero Massif, Kola Peninsula. Our reason for selecting this target area is that on the same day, about 4 hours and 40 minutes after the Turkey earthquake, a moderate earthquake (m_b=4.2) occurred in this place. We will in the following show a number of figures illustrating the surface wave observations and the results from surface wave threshold monitoring using two different frequency bands.

Fig. 6.2.3 shows the locations of the station network, and the locations of the Turkey and Lovozero events.

The seismograms of the Turkey event as recorded at NOA, ARCES and SPITS are shown in Fig. 6.2.4. Different types of seismometers are used at these three stations;
NOA - KS54000, ARCES - KS36000, SPITS - CMG-3T, and the epicentral distance to the three stations are 23.4, 28.9, and 37.9 degrees, respectively. Notice that the surface wave observations at ARCES are clipped.

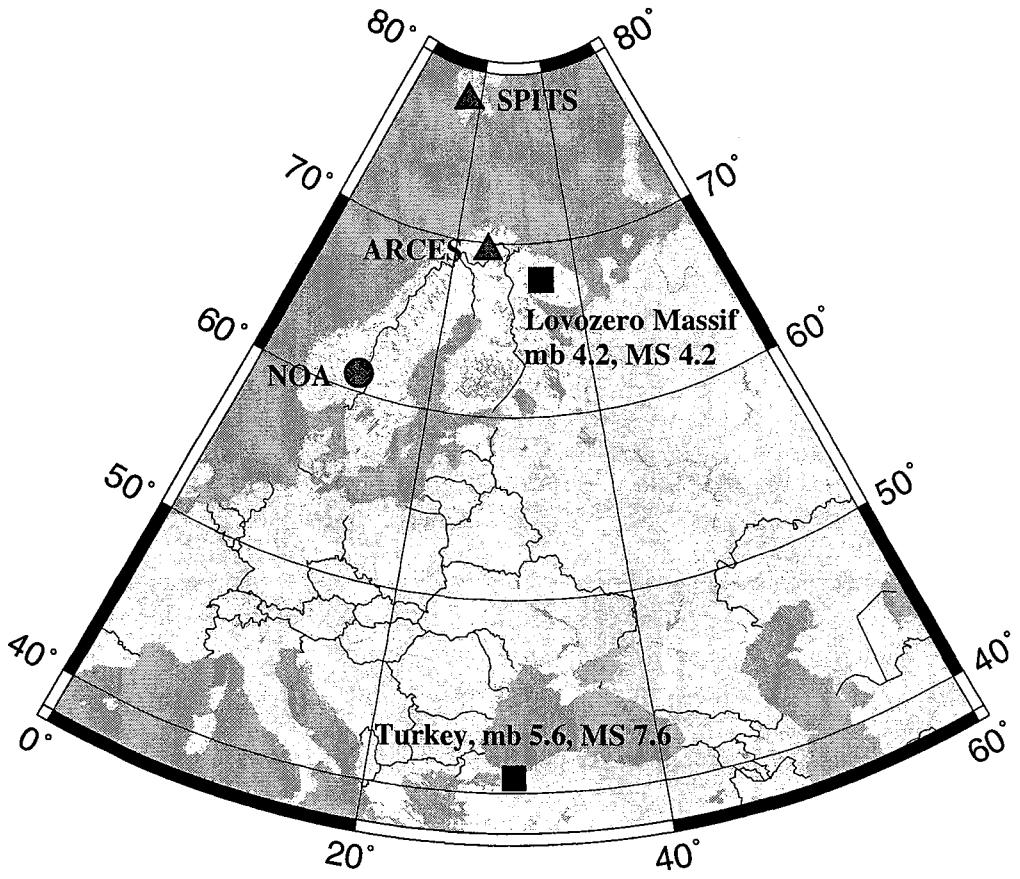

Fig. 6.2.3. Map showing the locations of the station network, and the Turkey and Lovozero events.

Fig. 6.2.5 shows the same time interval as in Fig. 6.2.4, but now with simulated KS36000 traces at NOA and SPITS. These are the data used for magnitude estimation at the PIDC. Band-pass filtered recordings of the Lovozero event are shown in Figs. 6.2.6 and 6.27. In the 17 - 24 s band (Fig. 6.2.6), the Rayleigh waves have a low SNR and is only visible at ARCES and NOA. In contrast, clear Rayleigh waves are seen at all stations in the 8 - 12 s period band (Fig. 6.2.7). The epicentral distance to ARCES, SPITS and NOA are 3.7, 11.5 and 12.1 degrees, respectively. Due to differences in the crustal and upper mantle structures, surface waves arrive later at SPITS than at NOA.

The NOA array consists of seven broad-band sensors deployed over an aperture of approximately 60 km. The surface waves from the Lovozero event arrive at NOA with an estimated back-azimuth of 42.4 degrees and an apparent velocity of 3.2 km/s. For the threshold monitoring experiment we beamform the NOA data using the estimated back-azimuth and slowness, resulting in improved SNR in both frequency bands. Based on 20 s Rayleigh wave observations at NOA and the ESDC array in Spain, we estimate a surface wave magnitude of 4.2 of the Lovozero event, using the relation of Rezapour and Pearce (1998).

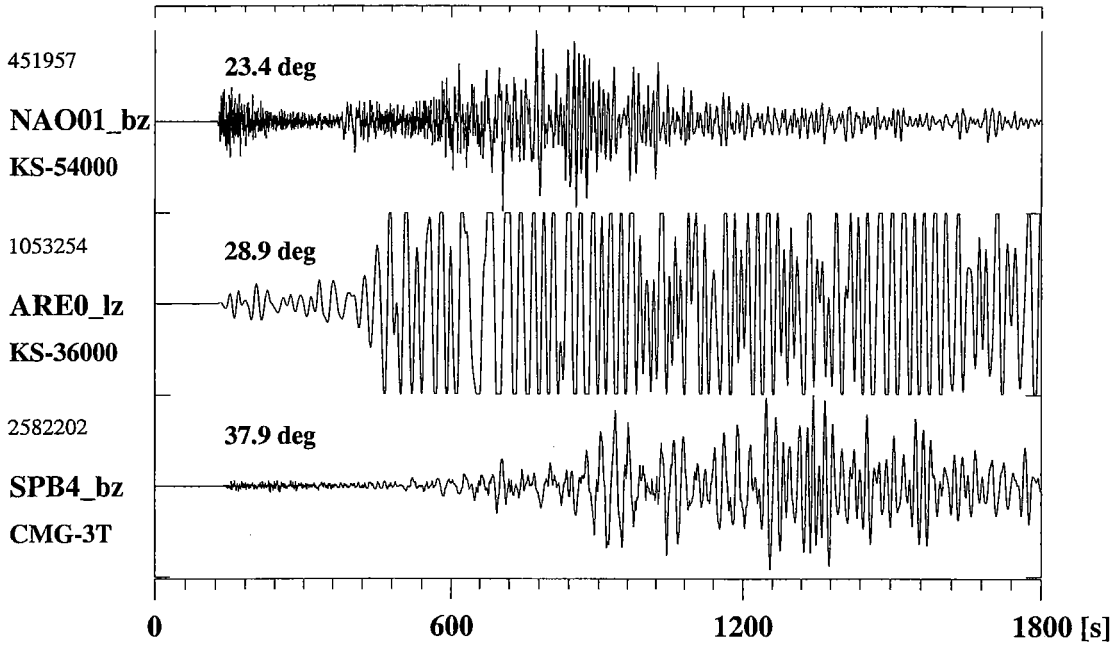

Fig. 6.2.4. NOA, ARCES and SPITS recordings of the Turkey event. Different types of seismometers are used; NOA - KS54000, ARCES - KS36000, SPITS - CMG-3T. The epicentral distances are given above each trace.

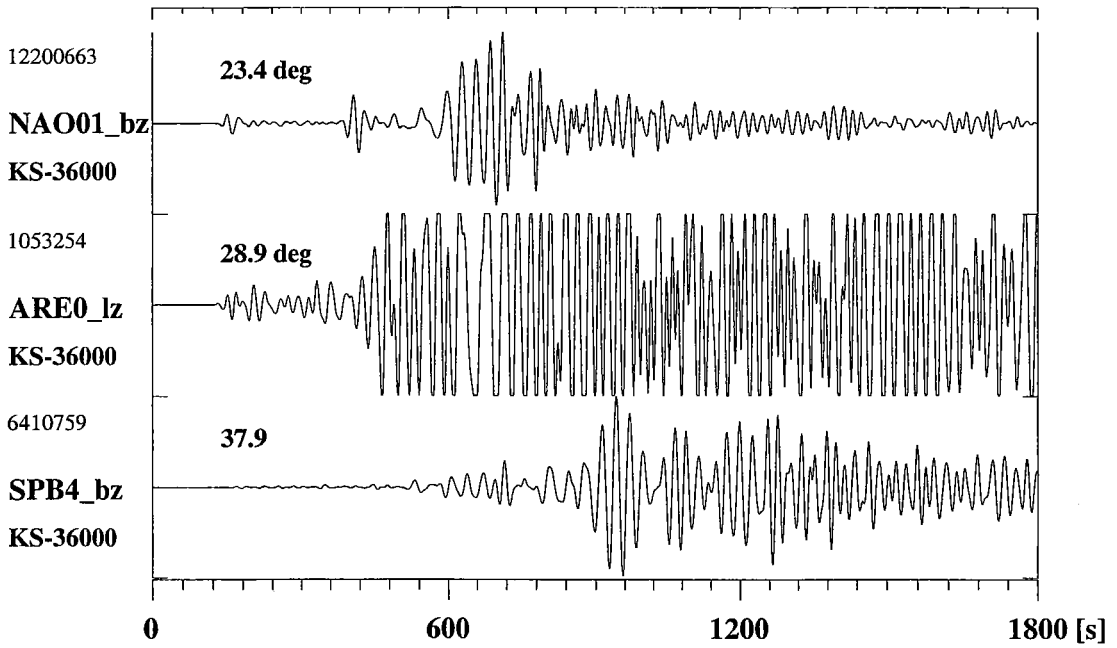

Fig. 6.2.5. Simulated KS36000 traces at NOA and SPITS for the Turkey event. The ARCES recording is shown in its original form (KS36000).

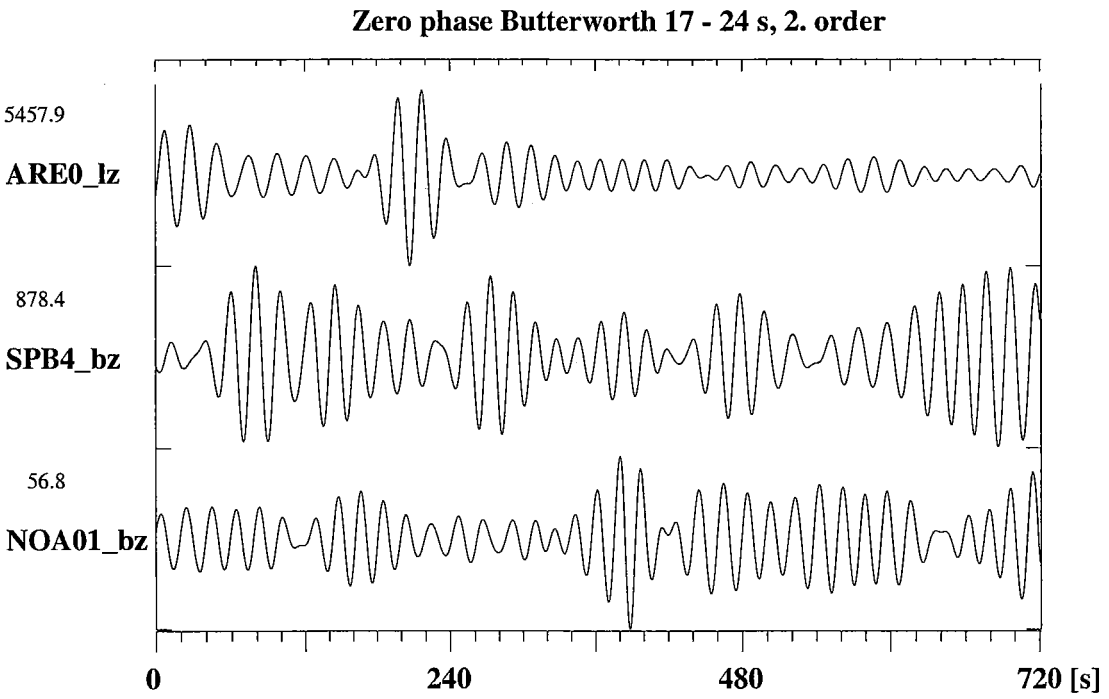

Fig. 6.2.6. Bandpass filtered (17 - 24 s) recordings of the Lovozero event.

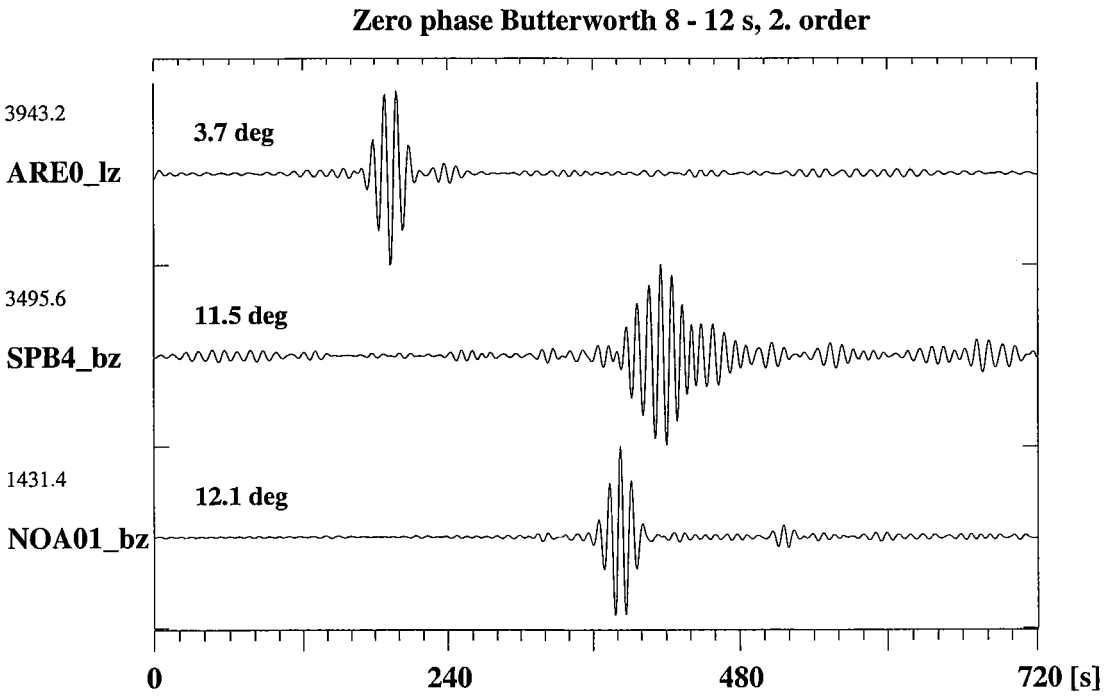

Fig. 6.2.7. Bandpass filtered (8 - 12 s) recordings of the Lovozero event. The epicentral distances are given above each trace.

Using the site-specific threshold monitoring approach for the location of the Lovozero event, we have derived processing parameters such as travel-times, STA lengths, and amplitude-magnitude relations from the actual ARCES, SPITS and NOA observations. The threshold processing results in the "standard" PIDC frequency band (17-24 s) are shown in Fig. 6.2.8. We see that the surface waves from the Lovozero event are effectively masked by the coda/aftershocks of the Turkey earthquake

However, in a more "high frequency" filter band (8-12 s) the surface waves from the Lovozero event stand out very clearly, see Fig. 6.2.9. This shows that "high frequency" processing of surface waves at regional distances can significantly improve detectability by suppressing the longer period energy from interfering distant earthquakes. Fig. 6.2.10 compares the threshold monitoring results for both frequency bands (17-24 and 8-12 s) for a 10 hour time period. This clearly illustrates that the amplitudes of surface wave coda of the Turkey event decay much more rapidly at higher frequencies.

Discussion

The continuous assessment of upper limits on surface wave magnitudes as described in this paper is an entirely new application of the Threshold Monitoring technique. Our results so far must be considered only as a preliminary indication of the potential of the method when applied to long-period seismic recordings, but it is already clear that there are significant possibilities for developing the TM process into a useful monitoring tool for surface waves.

In this study, we have used the three IMS arrays ARCES, NOA and SPITS, and applied a site-specific technique to investigate the threshold trace during a large earthquake sequence. A natural follow-up of this work would be to include additional long-period and broadband IMS stations for the same time interval, in order to assess the improvements in monitoring capability when using a network with better azimuthal coverage. It would also be interesting to steer the threshold beam to other sites, including the site of the earthquake sequence (Turkey), in order to assess the possibility for obtaining magnitude estimates (or upper limits) for individual aftershocks in the sequence.

An important result of this initial study is the demonstration of the significant benefits of using a shorter period band (8-12 seconds) instead of the traditional processing band (17-24 seconds) for processing surface waves at regional distances during an aftershock sequence. In future work, we will investigate further whether the use of this shorter period band could be applicable also during "normal" background noise conditions. In an operational setting, it is clearly an advantage to use a fixed frequency band for each station-site combination, but it requires a careful assessment of the relations between surface wave magnitudes calculated in different frequency bands.

As in the short period case, there is a tradeoff between optimizing the TM process for site-specific studies and developing a more general TM application for global surface wave monitoring. Among the main issues is the sharpness of the beam lobe, which depends upon the filter setting, the STA time windows and the tolerance for travel-time deviations. Another issue is the need for regional corrections, which may be greater than in the short-period case. For example, the significant difference between oceanic, continental and combined oceanic-continental paths are important for surface wave propagation, but have little or no counterpart in analyzing short-period P and S waves.

Since a main purpose of the MS measurements is to provide a basis for MS:mb screening (and discrimination), it is important to assess the effects of using shorter period surface waves on the MS:mb discrimination potential. Recent studies in the European Arctic (Krementetskaya et. al., 1998) have demonstrated some promising results using regional LP data from the Apatity long-period station for historic earthquakes and explosions in this region, including past nuclear explosions at Novaya Zemlya. This type of studies should be continued, using available regional recordings for earthquakes and underground nuclear explosions in various regions of the Earth.

T. Kværna
L. Taylor
J. Schweitzer
F. Ringdal

This work is conducted under contract DSWA01-97-C-0128

References

E.Kremenetskaya, V.Asming, Z. Jevtjugina and F. Ringdal (1998). Study of surface waves and Ms:mb using Apatity LP recordings. *Semiannual Technical Summary 1 April - 30 September 1998,* NORSAR Sci. Rep. 1-98/99, Kjeller, Norway.

Rezapour, M. and R.G. Pearce (1998): Bias in Surface-Wave Magnitude M_S due to Inadequate Distance Corrections. *Bull. Seism. Soc. Am.*, **88**, 43-61.

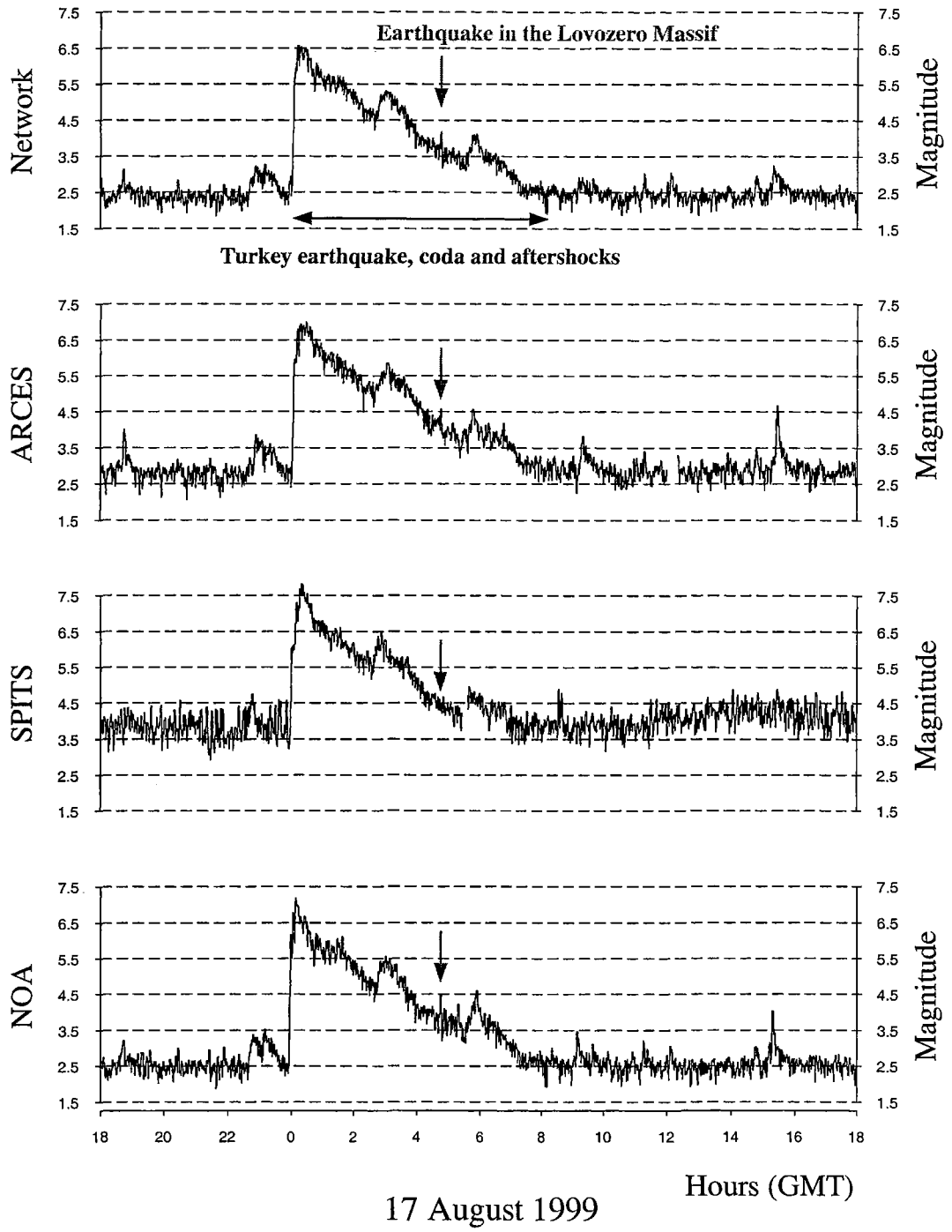

Fig. 6.2.8. Surface threshold monitoring for the location of the Lovozero event for 17 August 1999, using data filtered between 17 and 24 s. The lower three traces represent thresholds (upper 90% magnitude limits) obtained for each of the three stations, whereas the top trace shows the combined network thresholds. The peaks corresponding to the Lovozero event are indicated on each trace.

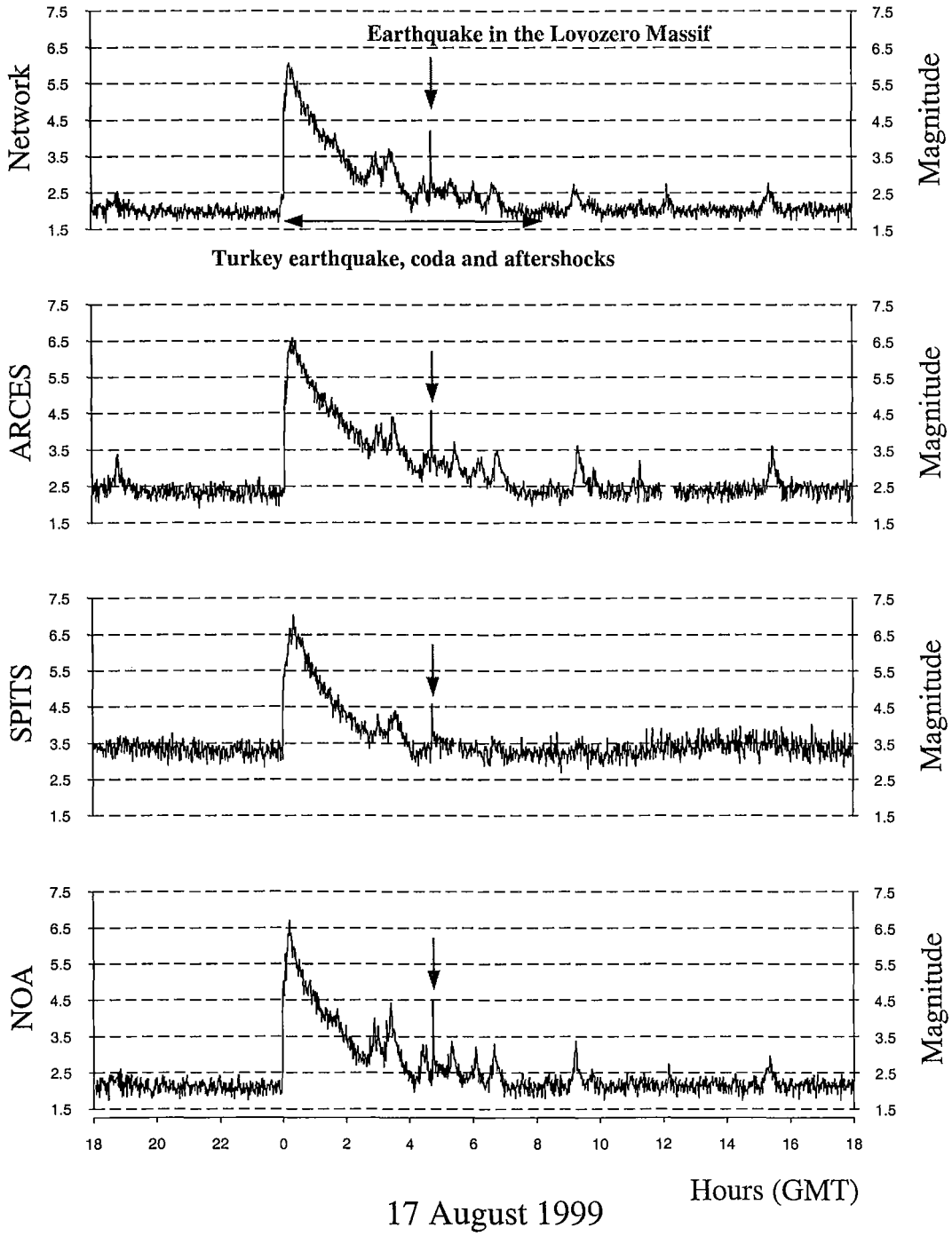

Fig. 6.2.9. Surface threshold monitoring for the location of the Lovozero event for 17 August 1999, using data filtered between 8 and 12 s. The lower three traces represent thresholds (upper 90% magnitude limits) obtained for each of the three stations, whereas the top trace shows the combined network thresholds. The peaks corresponding to the Lovozero event are indicated on each trace.

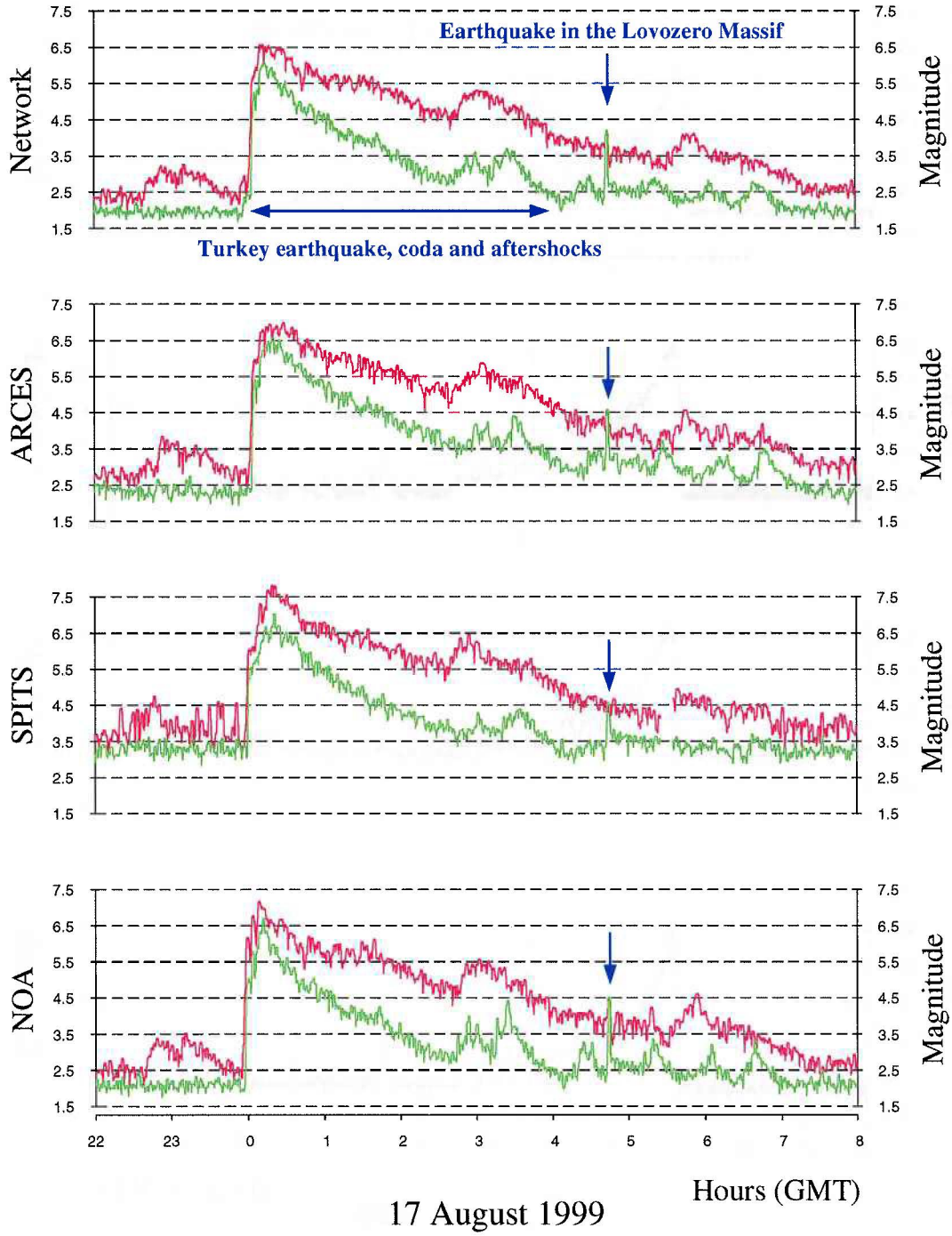

Fig. 6.2.10. Comparison between surface wave threshold monitoring using two different filter bands; red: 17 -24 s, green: 8-12 s. See captions of ***Figs. 6.2.8*** *and* ***9*** *for details.*